Model Extraction From Clinical Data Subject to Large Uncertainties and Poor Identifiability

Clara M. Ionescu, *Senior Member, IEEE*, Robin De Keyser, Dana Copot, Erhan Yumuk, Amani Ynineb, Ghada Ben Othman, and Martine Neckebroek

Abstract—**This letter presents an extension to system theory as a novel approach to provide models from clinical data under large uncertainty and poor identifiability conditions. These difficult conditions are often present in medical systems due to ethical, safety and regulatory limitations regarding application of persistent drug-related excitation to human body. Furthermore, drug-dose effect relationship is of particular challenge due to large inter- and intra- patient variability. This is strengthened by the lack of suitable instrumentation to measure the necessary information, rather making available inferences and surrogate metrics. A notable advantage of the proposed approach is its robustness to uncertainty. The efficacy of our approach was examined in clinical data from patients monitored during induction phase of target controlled intravenous anesthesia. The proposed method delivered models with physiological explainable parameters and suitable for closed loop control of anesthesia.**

Index Terms—**Anesthesia dynamics, identification, pharmacodynamic.**

I. INTRODUCTION

THE MEDICAL practitioner is facing today an unprecedented opportunity to leverage medical datasets to improve clinical tasks and potentially maximizing patient outcome. Modern statistical paradigms and artificial intelligence tools have a great added value in many cross-disciplinary fields, but medical field has proven conservative in welcoming revolutionary solutions [1], [2]. Multi-drug therapy is endorsed in research studies, but has not yet breakthrough into standard clinical practice due to limitations such as:

- lack of adequate instrumentation to provide the actual needed information in terms of specificity and accuracy,
- and lack of ethical and regulatory framework to maximize the potential of tools from control engineering.

Aleatory and epistemic uncertainties are fundamentally different in nature and require different approaches to resolve. Largely recognized by the control engineering community as the main origin of performance limitation of closed loop systems in anesthesia, is the aleatory uncertainty in patient models and epistemic uncertainty from actions of anesthesiologist and surgeon [3]. Due to presence of surgical disturbances, patient models can only be identified during the induction phase of anesthesia (in absence of disturbances) but are challenged by lack of persistent excitation. Several works endeavoured resolving this problem in data sets from anesthetized patients [4], [5]. Estimators are used to augment the information in model based control optimization algorithms [6], [7], but convergence to safe intervals is difficult [8]. Trajectory generation under constrained conditions and safety assurance convex optimization has shown promising results [9].

This letter develops a novel practical approach to reconcile the shortcomings from lack of good identifiability conditions when clinical data is used to develop models for control. Our approach consists of linear model extraction from data based observations combined with physiological insight to deliver minimal yet reliable models for closing the loop on control of anesthesia with multiple-input multiple-output (MIMO) variables. We use data information into filtering schemes for extracting physiologically based time constants and approximate dose-effect gain response. We make use of the analgesia region of interest during induction, as a case study, which is relevant for the identification problem. From real clinical data we illustrate pitfalls and caveats leading to practical solutions.

II. POPULATION BASED PHYSIOLOGICAL MODELS

Hypnosis regulation has the generic schematic representation of a two-drug pharmacokinetic (PK)–pharmacodynamic (PD) compartmental model given in Fig. 1. The control of this system has been largely addressed by the control community [4], [8], [10], [11].
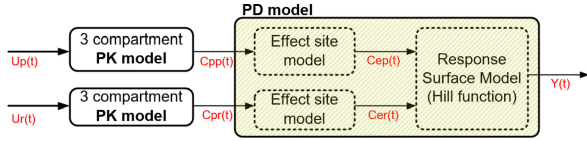
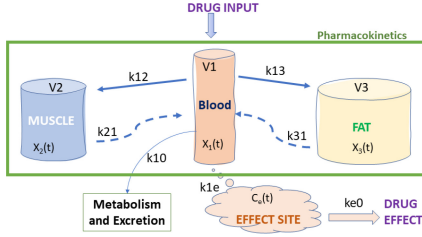Fig. 1. A schematic representation of a compartmental model for PK and PD with two inputs and one output.

Fig. 2. A schematic representation of variables into the compartmental model. The green block denotes the PK part of the model.

The PK model given in Fig. 2 can be expressed by means of concentrations in each compartment:

$$
\begin{pmatrix} \dot{x}_1 \\ \dot{x}_2 \\ \dot{x}_3 \end{pmatrix} = \begin{pmatrix} -(k_{10} + k_{12} + k_{13}) & k_{21} & k_{31} \\ k_{12} & -k_{21} & 0 \\ k_{13} & 0 & -k_{31} \end{pmatrix} \begin{pmatrix} x_1 \\ x_2 \\ x_3 \end{pmatrix} + \begin{pmatrix} \frac{1}{V_1} \\ 0 \\ 0 \end{pmatrix} u \tag{1}
$$

where the coefficients k_{ij} for $i \neq j$ denote the drug transfer frequency from the jth to the ith compartment expressed in 1/minute and $u(t)$ the infusion rate of the drug into the central compartment expressed in mg/minute or equivalently in ml/h. These coefficients are calculated from the biometric information (age, weight, height, gender) from the patient based on population based distributions. For Propofol see [12] and for Remifentanil see [13]. Typical time constants are about 2-5 minutes for the blood, approximately 20-40 minutes for the muscle and around 1 hour for the fat compartment.

The PD model is expressed as a hypothetic single compartment indicated as effect-site concentration C_e:

$$
\dot{C}_e(t) = k_{1e}x_1(t) - k_{e0}C_e(t) \tag{2}
$$

with $k_{1e} = k_{e0}$ and 0.456 for Propofol, respectively dependent on age A as follows $0.595 - 0.007 * (A - 40)$ for Remifentanil, in 1/minute. The single drug dose-effect relation between the effect site concentration C_e and the measured effect is modelled as a nonlinear sigmoid Hill curve scaled between 0%-100%, with 100% denoting no effect present:

$$
E(t) = E_0 - E_{max} \frac{C_e(t)^\gamma}{C_e(t)^\gamma + C_{50}^\gamma} \tag{3}
$$

where E_0 is the value when the patient received no drug; E_{max} is the maximum effect that can be achieved by the infusion of drug; C_{50} is the drug concentration at half of the maximum effect and γ is a parameter which together with the C_{50}
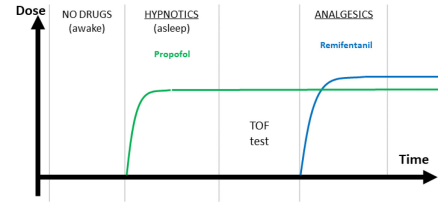

Fig. 3. A set of regimens for inducing general anesthesia preamble to surgery. TOF: train of four.

determines the patient sensitivity to the drug. In case of co-administration is used we have:

$$
E = E_0 - E_{max} \frac{\left(\frac{C_{er}(t)}{C_{50r}} + \frac{C_{ep}(t)}{C_{50p}} + \sigma \frac{C_{er}(t)C_{ep}(t)}{C_{50r}C_{50p}} \right)^\gamma}{1 + \left(\frac{C_{er}(t)}{C_{50r}} + \frac{C_{ep}(t)}{C_{50p}} + \sigma \frac{C_{er}(t)C_{ep}(t)}{C_{50r}C_{50p}} \right)^\gamma} \tag{4}
$$

where the initial and maximal effect scaling factors have been omitted and σ represents the degree of synergy between the drugs. The effect-site concentrations of Propofol and Remifentanil are denoted as C_{ep} in μg/ml and C_{er} in ng/ml and they act in synergy.

III. IDENTIFICATION FROM LOW-INFORMATION TIME-SERIES MEASUREMENTS

A. Clinical Protocol for Data Observations

Fig. 3 depicts a standard protocol of infusing hypnotic drug (Propofol) and opioid drug (Remifentanil) to the patient to achieve depth of hypnosis and analgesia. The output for hypnosis was BIS and the output for analgesia was measured by the AnspecPro device in four indices: AP1, AP2, AP3 and AP4, as defined in [14]. The clinical investigation involving human subjects was compliant with the regulatory framework stated in the European Regulation (EU) 2017/745. The study was approved by the Ethics Committee of Ghent University Hospital and the Federal Agency for Medicines and Health Products of Belgium FAGG (EC/BC-08020, FAGG/80M0840, EudraCT: CIV-BE-20-07-0342442020, clin-icaltrials.gov: NCT04986163, principal investigator: Martine Neckebroek). Details of included patients and available data are reported in [14].

In Fig. 3 we see the start of target controlled infusion (standard care infusion system for anesthesia) (TCI), an initial phase of no drug applied yet to patient (awake), followed by a phase of hypnotic drug infusion when the patient is set asleep. The test TOF (train of four) is a standard test consisting of four (electric) pulses to check the correct level of hypnosis in the state of the patient. Next phase is that of analgesic co-administration with hypnotic agent, achieving analgesia [10].

In such a clinical protocol, during the Hypnotics region, one can identify the true Hill curve corresponding, i.e., using (3). During the Analgesics region one can also update the gain using the surface model from (4), but keep in mind that this is in co-administration ode, whereas the 3D surface reduces to a 2D plot and piecewise linear over the limited variation of the output. Let us examine real data for a female of 36 years of age, with height 168 cm and weight 63 kg. The estimation uses a nonlinear least squares search function for steepest
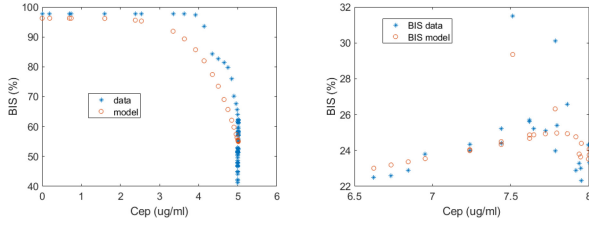
Fig. 4. Example of identified Hill curve using (3) (left) and surface model using (4) (right), from real patient data.
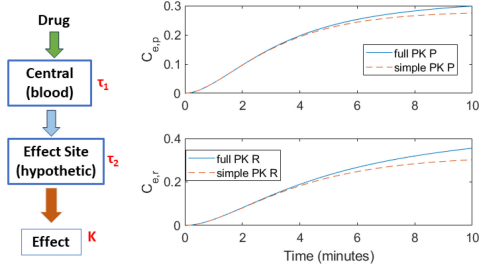

Fig. 5. Simplified model structure for identification (left). Step responses to test the rationale for simplified PK model. P denotes Propofol. R denotes Remifentanil (right).

gradient in MATLAB with function `lsqnonlin`, which gave the solution for the equation (3): $E0 = 96$, $E_{max} = 100$, $\gamma = 5.57$ and $C_{50p} = 12.03$. The result is given in Fig. 4-left. Identification of the surface model was performed also using a nonlinear least squares search function for steepest gradient in MATLAB with function `lsqnonlin`, which gave the solution for the equation (4): $E0 = 33$, $E_{max} = 100$, $\gamma = 18.57$, $\sigma = 2$ and $C_{50p} = 5.68$. Observe that due to synergy, the C_{50p} is now smaller than the value identified for the Hill curve single-drug effect, which again corresponds to theory. The result of identification from Fig. 4-right indicates the piecewise linear variation around the BIS=[22-26] interval.

B. Proposed Simplified Model Structure

Consider the compartmental model from Fig. 2, and the equations from (1). The time constants related to the measured time interval of the Analgesic region in Fig. 3 do not include effects of concentration profiles from muscle and fat compartments, as these are considerably larger than the time constant of the blood and the effect-site compartments. With this information at hand, we simplify and validate the model structure proposed in Fig. 5.

Theoretically, the transfer function model for the blood compartment is given by the formula:

$$M_{x_1,u} = \frac{\frac{1}{V1}}{s + k_{10} + k_{12} + k_{13}} \tag{5}$$

with $\tau_1 = 1/(k_{10} + k_{12} + k_{13})$ and for the effect-site compartment by:

$$M_{C_e,x_1} = \frac{k_{e0}}{s + k_{e0}} \tag{6}$$

with $\tau_2 = 1/k_{e0}$ and one may have a theoretical transfer function model of the simplified structure from Fig. 5 as series connection of (5) and (6) and extract the parameters τ_1, τ_2

and K, respectively. However, in [16] it has been shown that the model parameters from (6) are underestimated and data based identification is suggested to update this model. In this simplified model, there is no need to use the complex and nonlinear gains from (3) and (4) as they reduce to a constant K captured within the model (6).

C. Caveats and Pitfalls

Following the protocol depicted in Fig. 3, from the region denoted by *Hypnotics*, data is available to characterize the dose-effect relationship using (3), from which C_{50} and γ values for Propofol are identified [4], [10]. The region with TOF cannot be used for identification because this is a disturbance. Next, in the *Analgesics* region, we can identify the model from (4). However, the input is limited to a series of impulse and step like infusion rates. It is not possible to alter the clinical protocol as it affects the safety of the patient. The limitation in measurement time T_m (N samples) has serious consequences on the structure of the model to be identified. For a given bolus, this is equivalent to an impulse test, whereas for constant infusion rate, it is similar to a step test, both poor signal choice for identification procedures.

The problem can be stated as follows. Let a linear model of a discrete-time dynamical system be described by:

$$y(t) = \sum_{k=1}^{\infty} g(k)u(t-k) + v(t), \quad t = 1, 2, \ldots \tag{7}$$

where $y(t)$ and $u(t)$, for $t = 1, 2, \ldots$ are sequences of outputs and inputs, respectively, observed at a sampling interval T_s and $g(k)$ are impulse response coefficients. The additive disturbance $v(t)$ is unknown and has mixed stochastic and deterministic origin. We associate a transfer function or frequency function:

$$G(e^{j\omega}) = \sum_{k=1}^{\infty} g(k)e^{-jk\omega}, \quad -\pi \leq \omega \leq \pi \tag{8}$$

Supposing the impulse response coefficients $g(k)$ have been estimated from dataset

$$Z^N : y(t), u(t) \quad t = 1, 2, \ldots, N \tag{9}$$

measured from the true system, it corresponds to a transfer function

$$\hat{G}_N(e^{j\omega}) \tag{10}$$

where the emphasis lies on the fact that it is an estimate based on a limited set N of measurement samples.

Real data reveals that the expected response of effect site concentration and by extrapolation the analgesic level are not visible in the short window of the measured time interval. Identification algorithms applied directly to this data lead to model structures containing very fast time constant or integrator, as shown in our previous work [14]. This model structure is not explainable by physiologic insight and solutions are proposed hereafter.
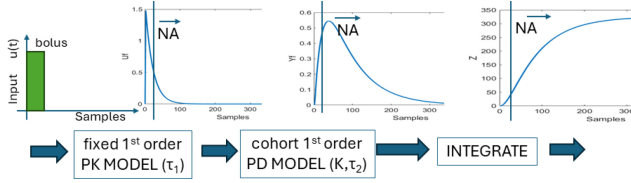
Fig. 6. Proposed methodology. Observe the drastic difference between available samples and not available (NA) needed samples.

Fig. 7. Simulated patient: numerical example of cohort preset values with N=500 samples (left) and N=50 samples (right) measurement time.

D. Proposed Identification Approach for K and τ_2

In this methodology we will generally work with signals (inputs and outputs) that may contain a deterministic component (e.g., from other physiological processes going on in the body during anesthesia), hence directly use the input drug $u(t)$ and the measured output effect $y(t)$, without other filtering or estimations. The signals will not be stationary stochastic processes, but we assume the limits exist:

$$\bar{\mathbb{E}}(y(t)u(t)) = \lim_{N\to\infty} \frac{1}{N}\mathbb{E}(y(t)u(t)) \qquad (11)$$

A first solution proposed here is to consider the Euclidean norm as a tool to extract the gain of the system and use it as calibration to the PK model calculated from biometric data of patient. Linear PK models defined in (1) with biometric parameters have essentially the same bandwidth, with small, non-significant variations in the time constants. However, a large variability has been observed and analysed in the dose-effect nonlinear gain expressed in (3) and (4) [18]. The simplified model given by series connection of (5) and (6) can be then fixed from PK model and only calibrated for patient individual gain from N data observations with:

$$K \approx \frac{\|y(kT_s)\|^2}{\|u(kT_s)\|^2} \qquad (12)$$

for $k = 1..N$ samples, where the $\|\cdots\|$ denotes the Euclidean norm of the signals which is positive definite.

The limitation of (12) is that it does not take into account dynamic model mismatch. A second solution proposed here is based on the classical signal definition as in (7) and summarized in Fig. 6, where zones are indicative of the missing signal information (not available NA) due to replacing measurement time $t \to \infty$ by a rather limited $t \to T_m$. Recalling Fig. 5, with the real input $u(t)$ and using (5), we obtain a filtered input $Uf(t)$. This is the input for identifying the effect site compartment (K, τ_2). For the time T_m measured for the discretized N signal samples with sampling period T_s, we have:

$$S1_{coh} = \sum_{k=1}^{N} Yf(kT_s) / \sum_{k=1}^{N} Uf(kT_s) \qquad (13)$$

and since the $Yf(t)$ is the actual measured impulse response of filtered bolus type input $Uf(t)$, in the limit for $t \to \infty$ this is the exact gain of the process. Next, having the impulse response of a first order systems described generically by $y(t) = Ke^{-t/\tau}$, let us integrate for $t \to T_m$, and obtain a signal $Z(t)$. The area of this response will change as a function of the time constant τ of the system but also on the gain. Let
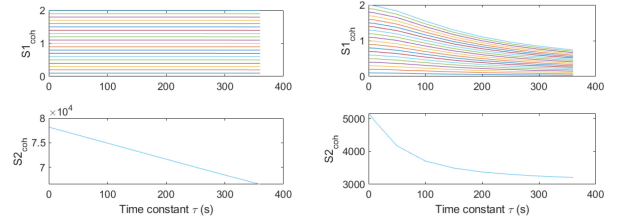
K be the end value of this response and it follows that the area under the response is given by $\sum_{k=1}^{N}[K - Z(kT_s)]$. If we normalize the area by the gain obtained from (13) we have:

$$S2_{coh} = \sum_{k=1}^{N} Z(kT_s)/S1_{coh} \qquad (14)$$

which in the limit $t \to \infty$ only depends on the time constant of the process. Relation $S1_{coh}$ depends on both (K, τ_2).

To apply this method on real data in order to find the specific patient related values of (K^*, τ_2^*), the procedure can be applied as follows.

- *Step 1–offline:* generate the cohort sets $S1_{coh}$ and $S2_{coh}$ from preset and calibration values of (K, τ_2).

Notice that calculating $S1_{coh}$ and $S2_{coh}$ is dependent on the device used to monitor nociception during anesthesia, as the interval range of output values varies among instruments. In Fig. 6 the fixed transfer function is calculated using (5) in interval sets for cohort sets. The next steps are *online* executed and real measured data.

- *Step 2:* update the fixed transfer function with biometric coefficients and model equation from (5) to fix τ_1.
- *Step 3* replace signals $Uf(t)$ and $Yf(t)$ by *real data measured signals* and calculate a point $P1 \in S1_{coh}$ using (13) and $P2 \in S2_{coh}$ using (14).
- *Step 4* Intersection of $P1$ and $P2$ with the cohort sets allows extracting the solution (K^*, τ_2^*) for real patient.

Notice that the data based identified first order transfer function with (K^*, τ_2^*) corresponding to the effect site compartment in Fig. 5 and the linear approximation of gain includes any model mismatch coming from the transfer function calculated with biometric data. In other words, the proposed method gives a *calibration in terms of full PK-PD model for that specific patient.*

IV. RESULTS FOR REMIFENTANIL

A. Ideal Conditions: Effect of Measurement Time T_m

In ideal identification conditions no noise and measurement time $t \to \infty$, i.e., N=500 samples with $T_s = 5$ seconds, we have the following numerical example. A male patient 53 years of age, 186 cm height and 114 kg weight gives a fixed PK transfer function model as: $M_{x1,u} = \frac{0.1551}{s+0.009524}$. For preset interval values of (K, τ_2) we obtain the $S1_{coh}$ and $S2_{coh}$ depicted in Fig. 7-left where we see indeed that $S1_{coh}$ depends linearly with the gains K and $S2_{coh}$ depends linearly with time constants τ_2. When the measurement time is significantly
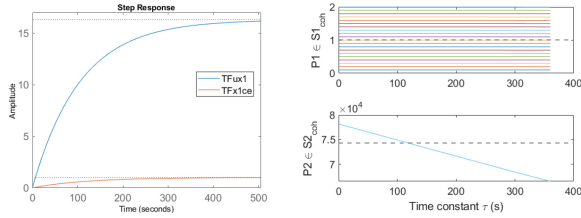
Fig. 8. Simulated patient with N=500 samples: the theoretical step responses and the identified (K^*, τ_2^*).
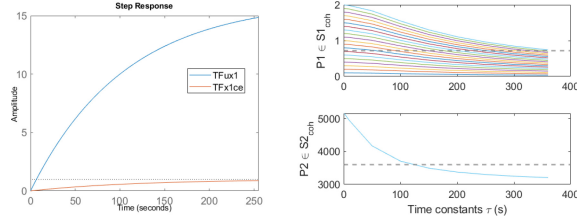

Fig. 9. Simulated patient with N=50 samples: the theoretical step responses and the identified (K^*, τ_2^*).
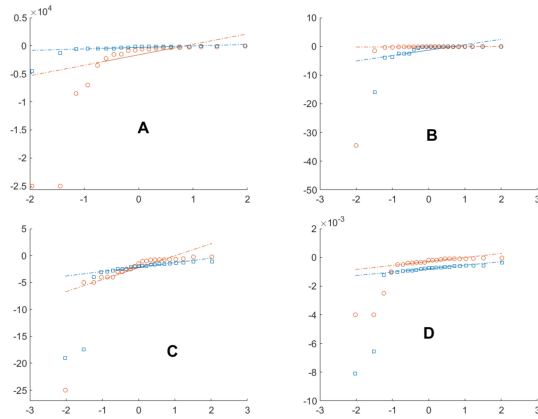

Fig. 10. Quantile regression plots for estimated gains K using model (10) depicted by red circles and estimated gains using model (12) depicted by blue squares. The horizontal axes are standard normal quantiles, whereas vertical axes are those given by the evaluated samples. The labels correspond to A - AP1, B - AP2, C - AP3, D - AP4, as developed in [14].

smaller, N=50 samples, this dependence becomes nonlinear, as in Fig. 7-right.

For N=500 samples, the theoretical step responses of $M_{x_1,u}$ and M_{C_e,x_1} with visible corresponding time constants are given in Fig. 8-left. The proposed method finds the true solution to (K^*, τ_2^*) as visible in Fig. 8-right, for PD transfer function model $M_{C_e,x_1} = \frac{0.0084}{s+0.0084}$ with $K^* = 1$ and $\tau_2^* = 119.0476$ seconds. For N=50 samples, the theoretical step responses of $M_{x_1,u}$ and M_{C_e,x_1} with corresponding time constants are given in Fig. 9-left. Also in this case, the proposed method gives the true solution for (K^*, τ_2^*) as visible in Fig. 9-right.

B. Real Data

1) Estimating K With (10) and (12): Estimations for gain using least squares estimation algorithm with (10) and the Euclidean norm with (12) have been compared using quantile regression algorithm and reported in Fig. 10 for all four
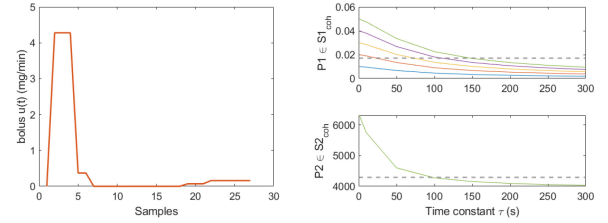

Fig. 11. Real data patient. Applied bolus type input (left) and identified (K^*, τ_2^*) solution (right).
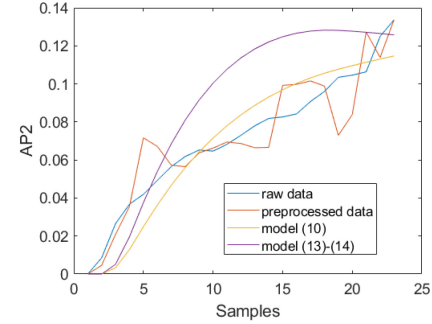

Fig. 12. Validation of model output for bolus type input against real data from patient.

output signals (i.e., AP1, AP2, AP3 and AP4) measured by the AnspecPro (AP) monitor from 23 patients described in detail in [14]. It can be observed that the procedure using (12) consistently provides a better fit to the normal distribution across all plots. The data points are either close to or follow the reference line well, which is indicative of normal distribution properties. Procedure using (10) more often deviates from the reference line, indicating that the data it produces does not conform as closely to a normal distribution. Most consistent distributions are observed for plot B, suggesting index AP2 is best candidate as output variable. These conclusions are in line with those reported in [14] and with real data based nonlinear surface model identification reported in [19].

2) Estimating K With (13) and τ_2 With (14): Consider applying the proposed solution on real data measured from a patient with the index AP2 from the AnspecPro monitor in region Analgesia from protocol depicted in Fig. 3. A female patient with biometrics: 42 years of age, 168 cm height and 70 kg weight, gives the fixed model $M_{x_1,u} = \frac{0.2154}{s+0.01702}$. The bolus infusion for Remifentanil in the Analgesic region is depicted in Fig. 11-left. The corresponding solution for the proposed method is given in Fig. 11-right. The comparison of responses using model (10) and the model extracted with proposed method is given in Fig. 12.

The difference between the result obtained by the classical model estimations (10) and the result using the proposed method is not immediately obvious. However, when examined in detail, we see indeed that due to limited data availability, the transfer function estimated with (10) is $M_{C_e,u} = \frac{1.5}{22500s^2+500s+1}$, which gives a pole location at -0.0022 (acts similar to an integrator) and another pole at -0.02. With the proposed method, we have the model $M_{x_1,u}$ from biometric data with pole at -0.017 and the estimated model $M_{C_e,x_1} =$

Model	τ_1 (s)	τ_2 (s)
(10)	35± 19.04 (27.75,45.09)	250 ±248.84 (201.96, 428.51)
(5)-(6)	65.14±18.29(59.85,76.51)	111.31±27.91(102.52,127.93)
(13)-(14)	65.14±18.29(59.85, 76.51)	91±31.04(75.80,104.06)

$\frac{0.05}{103s+1}$ with pole at -0.01, both values close to expected physical dynamics. The results obtained from 23 patients are summarized in Table I.

C. Discussion

In practice, a closed loop can be started with PK-PD models from literature and updated as the real data becomes available, in absence of disturbance and during intervals where input-output signals can be used for identification. The simplified model is indeed suitable for the closed loop since the larger time constants from the muscle and fat compartment are beyond the usual prediction horizon used in clinical practice of 10 minutes. Their effect is tackled the loop integrator which is present in all closed loop controls. The idea is to perform a first part of the model identification from the PK model part based on the biometric data. Here is not important which PK model definition is used from literature, since any uncertainty left over in the actual true patient model will be identified in the PD part of the model, ie a linear gain and time constant. The linear gain identified here is justified since it will be mostly used during maintenance phase of anesthesia, when the output remains around the steady state values. The identification of the PD model to the actual data available during the induction phase can be considered as a calibration method.

From Table I we observe that the model estimations using (10) have a dominant and far away pole, resulting in a fast and 5-10 times slower time constant. Our method provides a fixed pole from biometrics PK model for patient and an identified pole corresponding to physical time constants of effect-site compartment. A difference is observed between the calculated and the estimated time constant τ_2, suggesting that calibration to the real patient response is indeed meaningful to consider.

By generic definition, all models are bad, since they all contain uncertainty. The data is poor in richness, length and rather corrupted by artefacts in such a complex environment. Providing the controller with updated values of patient model it increases the potential of the control performance and reduces the uncertainty in the model. To summarize, this letter introduced an extension to system theory for allowing identification of simple yet effective transfer function models under poor identifiability conditions. Validation on real data indicates the relevance of the proposed approach.

ACKNOWLEDGMENT

REFERENCES

[1] J.-O. Hahn and O. T. Inan, "Physiological closed-loop control in critical care: Opportunities for innovations," *Progress Biomed. Eng.*, vol. 4, no. 3, 2022, Art. no. 33001, doi: 10.1088/2516-1091/ac6d36.

[2] M. Viceconti, M. De Vos, S. Mellone, and L. Geris, "Position paper from the digital twins in healthcare to the virtual human twin: A moonshot project for digital health research," *IEEE J. Biomed. Health Inf.*, vol. 28, no. 1, pp. 491–501, Jan. 2024.

[3] J. M. Gonzalez-Cava et al., "Robust PID control of propofol anaesthesia: Uncertainty limits performance, not PID structure," *Comput. Method. Program. Biomed.*, vol. 198, Jan. 2021, Art. no. 105783.

[4] K. Moussa, B. Aubouin-Pairault, M. Alamir, and T. Dang, "Data-based extended moving horizon estimation for MISO anesthesia dynamics," *IEEE Control Syst. Lett.*, vol. 7, pp. 3057–3059, 2023, doi: 10.1109/LCSYS.2023.3291665.

[5] A. Tivay and J.-O. Hahn, "A population-informed particle filter for robust physiological monitoring using low-information time-series measurements," *IEEE Trans. Biomed. Eng.*, vol. 70, no. 8, pp. 2298–2309, Aug. 2023, doi: 10.1109/TBME.2023.3241957.

[6] N. Paolino, M. Schiavo, N. Latronico, M. Paltenghi, and A. Visioli, "PKPD model based design of PID control for closed loop anesthesia," *IFAC J. Syst. Control*, vol. 27, no. 1, 2024, Art. no. 100247.

[7] B. Aubouin-Pairault, M. Fiacchini, and T. Dang, "Comparison of multiple Kalman filter and moving horizon estimator for the anesthesia process," *J. Process Control*, vol. 136, no. 2, 2024, Art. no. 103179.

[8] W. Yin, A. Tivay, H. K. Fathy, and J.-O. Hahn, "Hemodynamic safety assurance in closed loop controlled critical care: Hemorrhage resuscitation and sedation case study," *IEEE Control Syst. Lett.*, vol. 7, pp. 709–714, 2023, doi: 10.1109/LCSYS.2022.3220188.

[9] D. Malyuta et al., "Convex optimization for trajectory generation," *IEEE Control Syst.*, vol. 42, no. 5, pp. 40–113, Oct. 2022, doi: 10.1109/MCS.2022.3187542.

[10] D. D. Huff, M. Fiacchini, T. Dang, and T. Alamo, "Optimized coadministration of propofol and remifentanil during the induction phase of total intravenous anesthesia with statistical validation," *IEEE Control Syst. Lett.*, vol. 8, pp. 193–198, 2024, doi: 10.1109/LCSYS.2024.3359529.

[11] M. Schiavo, F. Padula, N. Latronico, M. Paltenghi, and A. Visioli, "Individualized PID tuning for maintenance of general anesthesia with propofol and remifentanil coadministration," *J. Process Control*, vol. 109, pp. 74–82, Jan. 2022

[12] T. Schnider et al., "The influence of method of administration and covariates on the pharmacokinetics of propofol in adult volunteers," *Anesthesiology*, vol. 88, no. 5, pp. 1170–1182, 1998.

[13] C. Minto et al., "Influence of age and gender on the pharmacokinetics and pharmacodynamics of remifentanil, part-I: Model development," *Anesthesiology*, vol. 86, no. 1, pp. 10–23, 1997.

[14] C. M. Ionescu et al., "Development, validation and comparison of a novel nociception/anti-nociception monitor against two commercial monitors in general anesthesia," *Sensors*, vol. 24, no. 7, p. 2031, 2024.

[15] A. D. Raval, J. Uyei, A. Karabis, L. D. Bash, and S. J. Brull, "Incidence of residual neuromuscular blockade and use of neuromuscular blocking agents with and without antagonists: A systematic review and meta-analysis of randomized controlled trials," *J. Clin. Anesth.*, vol. 64, Sep. 2020, Art. no. 109818.

[16] Y. Wahlquist, A. Gojak, and K. Soltesz, "Identifiability of pharmacological models for online individualization," *IFAC-PapersOnLine*, vol. 54, no. 15, pp. 25–30, 2021.

[17] C. M. Ionescu, J. T. Machado, R. De Keyser, J. Decruyenaere, and M. Struys, "Nonlinear dynamics of the patient's response to drug effect during general anesthesia," *Commun. Nonlin. Sci. Numer. Simul.*, vol. 20, no. 3, pp. 914–926, 2015.

[18] R. De. Keyser, D. Copot, and C. Ionescu, "Estimation of patient sensitivity to drug effect during propofol hypnosis," in *Proc. IEEE Int. Conf. Syst, Man, Cybern.*, Hong Kong, China, 2015, pp. 2487–2491, doi: 10.1109/SMC.2015.435.

[19] E. Yumuk, D. Copot, C. M. Ionescu, and M. Neckebroek, "Data driven identification and comparison of full multivariable models for Propofol-Remifentanil induced general anesthesia," *J. Process Control*, vol. 139, Jul. 2024, Art. no. 103243, doi: 10.1016/j.jprocont.2024.103243.